Journal of Chromatography A, 1217 (2010) 715–721

Contents lists available at ScienceDirect

Journal of Chromatography A

journal homepage: www.elsevier.com/locate/chroma

Multi-wall carbon nanotubes bonding on silica-hydride surfaces for open-tubular capillary electrochromatography

Jian-Lian Chen*

School of Pharmacy, China Medical University, No. 91 Hsueh-Shih Road, Taichung 40402, Taiwan

ARTICLE INFO

Article history:
Received 12 August 2009
Received in revised form 1 December 2009
Accepted 2 December 2009
Available online 6 December 2009

Keywords:
Multi-wall carbon nanotube
Nucleosides
Open-tubular capillary electrochromatography
Silica-hydride
Stationary phases
Tetracyclines

ABSTRACT

Prepared multi-wall carbon nanotube (MWNT) materials, including untreated MWNT, HNO_3-treated MWNT and HNO_3-HCl-treated MWNT were covalently attached onto a silica-hydride-modified capillary by hydrosilation, using the abundant double bonds between the pentagon carbons in the MWNT structure. These MWNT-incorporated capillaries were characterized by SEM, ATR-IR and electroosmotic flow (EOF) measurements in phosphate buffers with a pH range of 3.7–9.3 and in the mixtures of acetonitrile modifier. The untreated capillary was assumed to carry some carboxylate groups formed on the non-acid-treated MWNTs, as it had higher EOF values than the hydride capillary. As the MWNTs were treated with HNO_3 and HCl solutions, the capillaries had increasingly higher EOF values. To examine the existence of an electrochromatography mechanism in the modified capillaries, a mixture of nucleosides and thymine was probed to check the velocity factor and retention factor. In addition to the π–π interaction between the probe solutes and the MWNT immobilized stationary phases; a reversed-phase mechanism could contribute to the chromatographic retention. For acidic tetracyclines, increasing the loadability of MWNTs resulted in a high retention factor and improved the separation resolution.

1. Introduction

As the core of capillary electrochromatography (CEC) is column preparation, the open-tubular (OT) style is a comparatively straightforward one; it does not require the fabrication of any frits for packed formats or blending of monomeric reagents with suitable porogens in precise proportions for monoliths [1–4]. However, OT-CEC suffers from a low phase ratio of available functional ligands attaching on the capillary wall. As such, etching the capillary wall surface and/or coating porous polymeric matrices are generally adopted methods to increase the loadability of phase materials [5,6]. Additionally, the nanoparticles exhibiting high surface area would also create efficient phases for OT-CEC after their non-covalent or covalent bonding onto the columns. There are examples in the literature of ultizing this process with latex [7], human very-low-density lipoprotein [8], high-density-lipoprotein [9], mesoporous silica [10], and titanium dioxide [11]. One popular nanomaterial is carbon nanotubes (CNTs), which have unique properties including high electrical conductivity, mechanical strength, and chemical stability [12,13]. In contrast to many studies and reviews concerning the use of CNTs as adsorbents [14,15], LC stationary phases [16], GC stationary phases [17] and EKC pseudo-stationary phases [18], only four papers on CEC stationary phases were found [19–22].

In general, non-covalent methods are simpler than covalent methods, but covalent methods provide a stronger and steadier incorporation of functional moieties onto the derived capillary wall surface. In two of the CEC papers on CNT-incorporated stationary phases, the negatively charged single-walled CNTs (SWNTs) were electrostatically adsorbed on the positively charged amine-based capillary by using either the simple acid-treated form [19] or blending in the monolithic monomers (vinylbenzyl chloride and ethylene dimethacrylate) [20]. Another paper also considered a non-covalent method where SWNTs conjugated with BSA proteins are physically encapsulated in the microchip electrophoresis channels through sol–gel condensation [21]. Another recent study seemed to use a covalent immobilization method [22]. However, the detailed chemistry dealing with the bonding between carboxylic multi-walled CNTs (MWNTs) and the glutaraldehyde-treated capillary following the silanization with the 3-aminopropyl triethoxysilane reagent was not unveiled.

We suggest the utilization of the double bonds within the CNTs structure as a reasonable approach to covalently attach the moieties onto the capillary wall. Carbon-atom pentagons at the curvature points in the CNTs are assumed to be involved in the π-bonds that break during the polymerization reaction [23,24].

* Tel.: +886 4 2205 3366; fax: +886 4 2203 1075.
E-mail address: cjl@mail.cmu.edu.tw.

0021-9673/$ – see front matter © 2009 Elsevier B.V. All rights reserved.
doi:10.1016/j.chroma.2009.12.018

According to work done over the last decade, Pesek et al. have developed a novel method that replaces approximately 95% of the Si–OH groups on the bare capillary with Si–H groups and further attaches desired organic moieties with carbon double-bond functionality to the hydride surface [25,26]. The reaction protocol, involving silanization and hydrosilation, leads to a stable Si–C bond between the capillary wall and the organic moiety. One of the primary advantages of this protocol is its versatility. Until recently, these hydride-based OT-CEC stationary phases included the attached moieties of diol, *n*-butylphenyl, cholesterol, *n*-C_5, and *n*-C_{18} [27,28,5]. Furthermore, we incorporate ionizable carboxylate ligands in with the hydride phases to enhance the EOF drive in CEC separation [29,30].

In this study, MWNTs treated by HNO_3 and then HCl were attached to a hydride-based surface. The complete capillary was characterized by the measurements of SEM and ATR-IR. Furthermore, the effect of the EOF on the changes in pH and acetonitrile volume percentage in the running buffers were recorded and tracked for each intermediate capillary between the silanization and hydrosilation of different acid-treated MWNTs steps. A mixture of nucleosides and thymine were probed to prove that the CEC mechanism existing in the MWNT immobilized capillary. Furthermore, a modified capillary with higher loading content of MWNTs was tried to separate tetracycline samples.

2. Experimental

2.1. Materials

Most chemicals used were of analytical or chromatographic grade. Purified water (18 MΩ cm) from a Milli-Q water purification system (Millipore, Bedford, MA, USA) was used to prepare samples and buffer solutions. All solvents and solutions for CEC analysis were filtered through a 0.45 μm cellulose ester membrane (Adventec MFS, Pleasanton, CA, USA).

2.1.1. Reagents

Triethoxysilane (TES), hexachloroplatinic acid (Speier's catalyst, H_2PtCl_6), cytidine (Cyd), guanosine (Guo), adenosine (Ado), thymidine (Thd), uridine (Urd), thymine (Thy), minocycline (MNC), and doxycycline (DC) were purchased from Sigma–Aldrich (Milwaukee, WI, USA). Tetrahydrofuran (THF) and ammonium hydrogen difluoridewere received from Acros (Thermo Fisher Scientific, Geel, Belgium). HPLC-grade acetonitrile (ACN), dimethylsulfoxide (DMSO), acetone, methanol, iso-propanol, dioxin, toluene, hydrochloric acid, sodium hydroxide, boric acid, sodium tetraborate, phosphoric acid, sodium dihydrogenphosphate, disodium hydrogenphosphate, tri-sodium phosphate, ammonium bicarbonate, and ammonium carbonate were supplied by Merck KGaA (Garmstadt, Germany). The MWNT materials were supplied by Conyuan Biochemical Technology (Taipei, Taiwan) and their specifications are: 20–40 nm for the main range of external diameter, 5–15 μm for the length, 95–98% for the purity volume, 40–300 m^2/g for special surface area, 2 wt% of amorphous carbon, and 0.2 wt% of ash.

2.1.2. Analytes

Cytidine (Cyd), guanosine (Guo), adenosine (Ado), thymidine (Thd), uridine (Urd), thymine (Thy), minocycline (MNC), and doxycycline (DC) were purchased from Sigma–Aldrich (Milwaukee, WI, USA). Methacycline (MTC) was received from Acros (Thermo Fisher Scientific, Geel, Belgium). Chlortetracycline (CTC) was obtained from Fluka (Sigma–Aldrich, Milwaukee, WI, USA). Stock solutions of samples were prepared in 0.2 mg/mL while nucleosides and thymine were dissolved in H_2O but tetracyclines in ACN/H_2O (1/1, v/v).

2.2. Instrumentation

The laboratory-built electrophoresis apparatus consisted of a ±30 kV high-voltage power supply (TriSep TM-2100, Unimicro Technologies, CA, USA) and a UV–Vis detector (LCD 2083.2 CE, ECOM, Prague, Czech). Electrochromatograms were recorded using a Peak-ABC Chromatography Data Handling System (Kingtech Scientific, Taiwan). The SEM images were acquired at an accelerating voltage of 3.0 kV by a Joel JSM-6700F Scanning Microscopy at National Chung Hsing University. The ATR-IR spectra were obtained by a Shimadzu Prestige-21 IR spectrometer, equipped with a single reflection horizontal ATR accessory (MIRacle, PIKE Technologies, WI, USA).

2.3. Preparation of capillary columns

The preparation of an etched silica-hydride phase was employed according to the previous description [29,30]. In brief, a new bare capillary column (Polymicro Technologies, Phoenix, AZ, USA) with 375 μm O.D. × 75 μm I.D. was treated with 1.0 M NaOH and successively washed with pure water, 0.1 M HCl, pure water and acetone. The washed capillary was then etched by ammonium hydrogen difluoride in methanol (5%, v/w) at 400 °C for 4 h. After cleaning out the nonreactive residue, the etched capillary was silanized by 1.0 M TES in dioxane for 1.5 h at 90 °C. Finally, the silanization was complete following a toluene rinse to prep the columns for the subsequent hydrosilation reaction with different MWNTs.

The first column used the original MWNT materials without any treatment, as received from the supplier. The second group of MWNTs was treated with HNO_3 (3.0 M) for 24 h at 60 °C. The third group was obtained from the further reflux of HNO_3-treated MWNTs in HCl (5.0 M) for 6 h at 120 °C. All three groups of MWNTs were dispersed in dioxane (1.0 mg/mL) and 2 mL of the dioxane solution was taken to be mixed with 70 μL of Speier's catalyst (H_2PtCl_6) in iso-propanol (10 mM). The hydrosilation occurred at 120 °C for 16 h after filling the mixture in a complete hydride-modified capillary. Finally, the three capillaries, labeled as SiH-CNT0, SiH-CNT1 and SiH-CNT2, respectively, were washed successively with dioxane, THF, and methanol for 30 min and then dried overnight under nitrogen flow at 20 psi. The recipe for the preparation of the forth column, SiH-CNT2×5, with HNO_3-HCl-treated MWNTs was the same as the above description, except the dioxane solution had a concentration of 5.0 mg/mL.

2.4. CEC conditions

The BGE used was ammonium carbonate, sodium phosphate and sodium borate buffer; DMSO was used as the neutral marker. At the end of analysis, the studied capillary was washed with methanol, pure water, and running buffer sequentially during the intervals between runs. Prior to a sample injection, a working voltage was applied for 5 min to condition the charge distribution in the column. The samples were injected by siphoning at a height difference and were detected by UV light absorption measurement at 214 nm for DMSO, 254 nm for nucleosides and thymine, and 355 nm for tetracyclines.

The optimized BGE, including the parameters of composition, pH value, and concentration, for the CEC separation of analytes were discussed in Sections 3.2 and 3.3, while the other conditions, such as applied voltage and hydrostatic sample injection, had been optimized at first and showed in the figure legend.

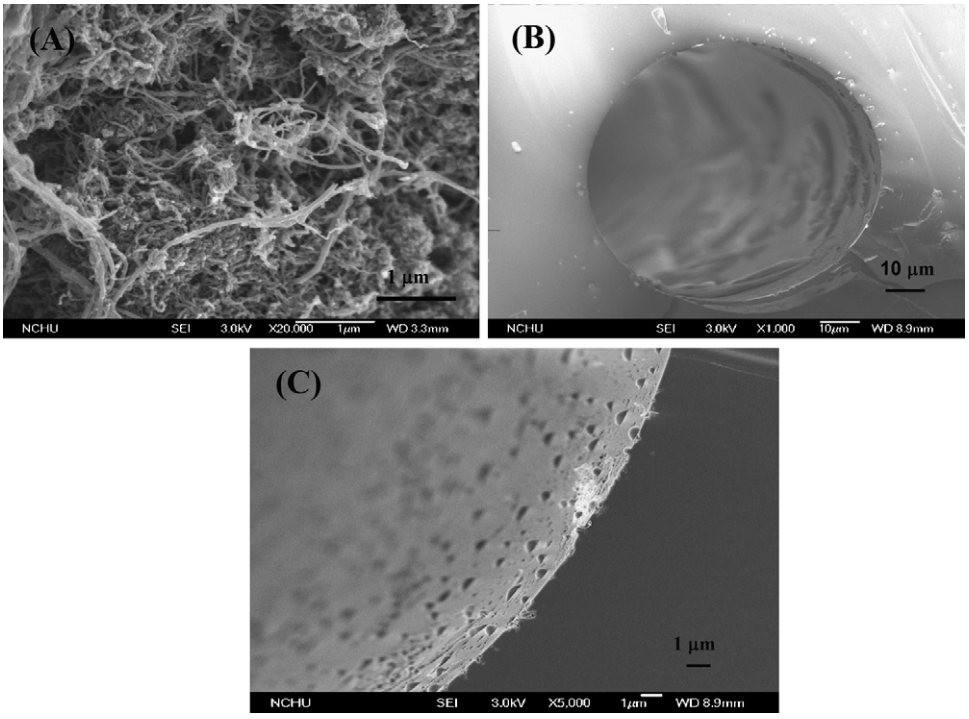

Fig. 1. SEM images. (A) Acid-treated MWNT; (B) cross-section of SiH-CNT2 capillary; (C) the magnification image of (B) around a cutting rim.

3. Results and discussion

3.1. Characterization of MWNT-modified capillaries

3.1.1. SEM images

The MWNT materials used in this study were treated in 3 M HNO_3, followed by a reflux process in 5 M HCl. After the acidic treatment and drying, the morphological appearance of the MWNT was as presented in the SEM image of Fig. 1(A). Although many nanotubes were clogged and formed in a mass, they will be dispersed in the dioxane medium. The SEM image in Fig. 1(B) demonstrates the completion of the MWNT spreading over the silica-hydride layer on the capillary wall surface. It is evident that colonies of MWNTs were strongly bonded on the inner surface of the completed capillary, SiH-CNT2, even though the capillary was washed with dioxane thoroughly for 1 h at 40 psi under ultrasonication. By comparison, no MWNT was found in the bare etched capillary, which was also loaded with acid-treated MWNTs and washed under ultrasonication. Being a 5× magnified picture of Fig. 1(B), Fig. 1(C) indicates some MWNTs located at the cutting rim and many traces of rough surfaces caused by the etching step for the modification of bare capillaries.

3.1.2. ATR-IR spectra

The ATR-IR spectra of the MWNT material treated with HNO_3/HCl and the finely ground power of a SiH-CNT2 capillary are shown in Fig. 2(A) and (B), respectively. A great difference between the two spectra is the Si–O stretching appeared at 1100 cm^{-1} in Fig. 2(B). However, the other peaks seem alike and show the characteristic absorption of CNT at 1520 cm^{-1} for conjugated C=C stretching [31], 1640 cm^{-1} for the non-conjugated C=C stretching [32], 1700 cm^{-1} for C=O stretching [22,32] and around 3500 cm^{-1} for –OH stretching [33] from the carboxyl groups introduced by the acid treatment. Carboxyl group was reported to be the product of nitric acid oxidation of CNT [22,32–34], although the oxidation reaction might produce other oxygen containing functional groups as reported for some carbon materials [35]. The spectrum of the MWNT material treated only with HNO_3 is not shown as it resembled Fig. 2(A) very much.

3.1.3. The EOF profiles upon buffer pH

Before applying the MWNT-modified capillaries to electochromatographic analyses, characterization of the EOF driven by these capillaries in different medium is necessary. The six curves shown in Fig. 3 illustrate the dependence of electroosmotic mobilities (μ_{eo}) on the pH levels of the phosphate buffer for an etched fused-silica capillary, a silanized (SiH) capillary and those derived from the hydrosilation of SiH capillaries with different MWNTs.

Details about the curve patterns of the etched capillary and the SiH one in the μ_{eo} vs. pH plot had been discussed in previous work [29]. Among of the discussion, one may notice that a hump appearing in the plot around pH 6–7 for etched capillaries could correlate with the existence and contribution of silanol groups

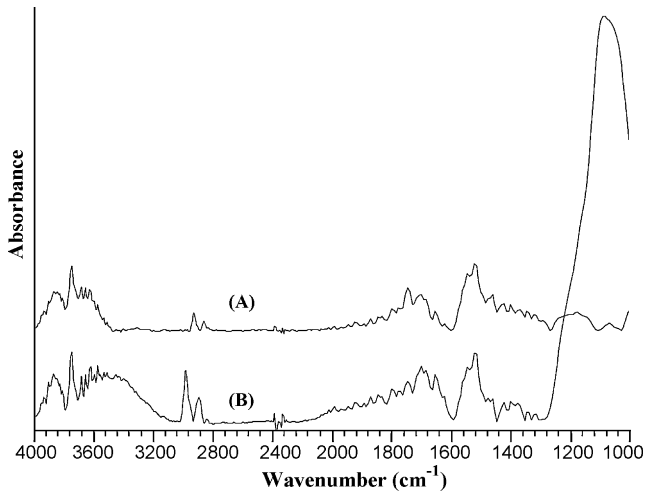

Fig. 2. ATR-IR spectra. (A) Acid-treated MWNT; (B) SiH-CNT2 capillary.

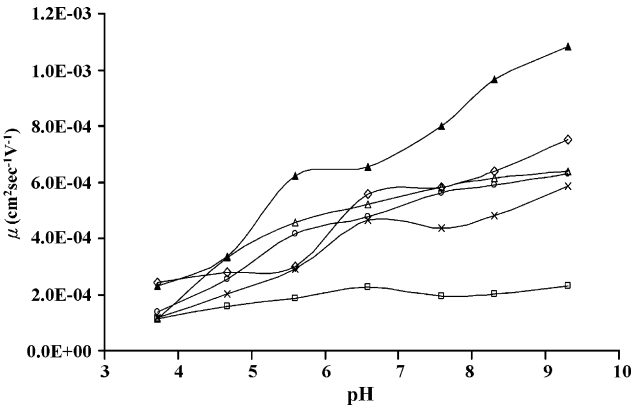

Fig. 3. Dependence of electroosmotic mobility on buffer pH. Column: (◊) etched capillary; (□) SiH; (×) SiH-CNT0; (○) SiH-CNT1; (△) SiH-CNT2; (▲) SiH-CNT2×5. Sample: DMSO; detection, 214 nm. Conditions: BGE, phosphate buffer, 50 mM; applied voltage, 20 kV.

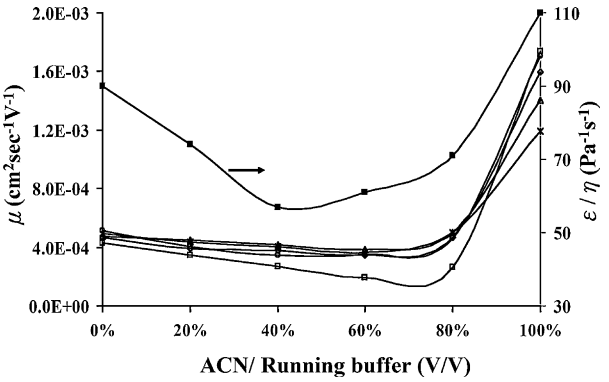

Fig. 4. Electroosmotic mobility as a function of ACN percentage in the phosphate buffer. Condition: BGE, mixing with phosphate buffer, pH 7.58, 10 mM, and ACN; applied voltage, 20 kV. Sample and column are the same as in Fig. 3. (■) denotes the ε/η values of the mixing buffer.

to the μ_{eo} values. This also happened to the untreated MWNT immobilized column, SiH-CNT0. However, the immobilization of untreated MWNT materials onto the SiH capillary through hydrosilation did raise the μ_{eo} values. These values for the SiH-CNT0 capillary are comparable to the report on the immobilized MWNT capillary, which underwent a carboxylation by the 3:1 concentrated H_2SO_4:HNO_3 mixture [22]. Some parts of MWNT materials built in the SiH-CNT0 capillary might have been oxidized to form certain carboxylate groups either prior to being received from the supplier or during the hydrosilation step.

Regarding the SiH-CNT1 and SiH-CNT2 capillaries, the oxidation occurred and the carboxylate groups were intentionally introduced to the HNO_3-treated MWNT macromolecules. Accordingly, the two capillaries had more chargeable carboxylate groups and exhibited higher μ_{eo} values than the SiH-CNT0 capillary. Furthermore, no hump is obviously found in the two curves showing similar patterns, so the influence of un-reacted silanol groups on the μ_{eo} values might be covered by the newly forming carboxylate groups. In addition, the SiH-CNT2 capillary used the MWNT materials that were further treated with HCl to remove the metal ions embedded in them [36]. These cations, derived from the catalyst for the synthesis of the MWNTs, reduce the negative charge density on the Stern layer and slow a cathodic EOF. For this reason, the μ_{eo} values of the SiH-CNT1 capillary without HCl-treatment are slightly lower than the SiH-CNT2 with HCl-treatment. However, these cations did not seem to heavily interfere with the ionization pattern of the ligands existing on the stationary surface of SiH-CNT1 capillary within the studied pH range.

The last curve, appearing at the topmost position in Fig. 3, shows that the highest density of surface charge among the modified capillaries resided in the SiH-CNT2×5 capillary. During the hydrosilation for the SiH-CNT2×5 column, the concentration of the acid-treated MWNT solution was five times (5 mg/mL) higher than that used for the SiH-CNT2 column (1 mg/mL). This change resulted in a higher loadability of ionizable carboxylate ligands, and also supported the influence of MWNT quantity on the reactivity of silicon hydride groups in the SiH capillary. Moreover, the SiH-CNT2×5 capillary will be a unique CEC column, as it has a sufficient amount of MWNT moieties to afford chromatographic selectivity and fast cathodic EOF to separate acidic analytes. The reproducibilities of fabricating capillaries were evaluated by the μ_{eo} values measured at pH 7.6 for five times in each of three newly prepared capillaries in the same format. The RSD values (n = 3) were 3.2% for the SiH-CNT0 column, 4.7% for the SiH-CNT1 column, 5.3% for the SiH-CNT2 column, and 5.1% for the SiH-CNT2×5 column, respectively. At the 95% confidence level, no difference between columns has been established.

3.1.4. The EOF profiles upon the ratio of ACN modifier

The effect of ACN in the buffer solution on the μ_{eo} values is highlighted in Fig. 4, which shows a minimum of EOF around 40–60% ACN content for various capillaries and also has concave curves [29,30,37,38]. The μ_{eo} values of the neutral solute DMSO did not simply increase with an increasing ratio of ACN in the eluent, acting as if a reversed-phase chromatography was not present at all. Apparently, these results were primarily due to a change in the ratio of dielectric constant to viscosity of the running buffer with an increasing ACN proportion from 0 to 100% (see the Y_2 axis in Fig. 4). This situation suggested that the DMSO solute was a good EOF probe and its chromatographic interaction with the MWNT immobilized phases could be ignored.

3.2. Separation of a mixture of nucleosides and thymine

Five nucleosides and thymine were used as probes to the CEC separation performance in the SiH-CNT0, SiH-CNT1, and SiH-CNT2 capillaries. For each capillary, experiments with a series of widely used CZE buffers, namely sodium phosphate, ammonium carbonate and sodium borate at a pH range of 8.5–10.5 and an ionic concentration range of 10–100 mM were primarily tried. The results achieved with a borate-based buffer system showed good peak shapes and resolution. The improved selectivity might be partly provided by the formation of complexes between the borate ions and the diol groups of the ribose units linked in the nucleosides [39,40]. Among the electrochromatograms, three obtained in the optimum conditions for each corresponding capillary are given in Fig. 5, which shows that the migration times of probe solutes were very dependent on the EOF magnitude. For electrophoretic separation, we employed a cathodic EOF and an anodic migration of solutes; the shorter migration times were measured in Fig. 5(C) conditions, where the EOF value was higher than the other two conditions. However, their migration orders were unaltered. These results may imply that the separation mechanism occurred in each CEC system was not very diverse. This situation especially happened to the SiH-CNT1 and SiH-CNT2 capillaries, where their optimum buffer was the same (i.e., same electrophoretic mobility, μ_{ep}) and phase property was similar (i.e., had a similar chromatographic retention). Differentiating between the electrophoretic and chromatographic contributions to the satisfactory separation is essential, particularly to this study, which focuses on the retention induced by MWNT.

Adopting the definition by Rathore and Horváth, measures of electrophoretic migration and chromatographic retention in CEC can be displayed as velocity factor (k''_e) and retention factor (k''),

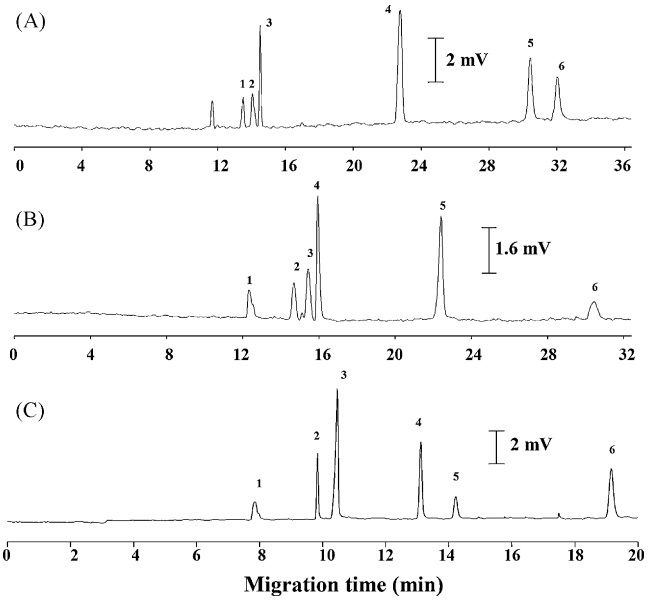

Fig. 5. Electrochromatographic separation of the mixture of nucleosides and thymine under the borate buffers without ACN modifier in various MWNT immobilized capillaries. Sample: concentration, 0.03 mg/mL; hydrostatic injection, 15 cm, 5 s; detection, 254 nm. Column and condition: (A) SiH-CNT0, 65.4 cm (60.4 cm) × 75 μm I.D.; BGE, pH 9.06, 0.05 M; applied voltage, 13 kV; (B) SiH-CNT1, 64.9 cm (60.0 cm) × 75 μm I.D.; BGE, pH 9.55, 0.03 M; applied voltage, 13 kV; (C) SiH-CNT2, 52.7 cm (47.7 cm) × 75 μm I.D.; BGE, pH 9.55, 0.03 M; applied voltage, 10 kV. Peak identification: (1) Thd, (2) Thy, (3) Ado, (4) Cyd, (5) Guo, and (6) Urd.

respectively [41,42]. In brief, they are expressed by Eqs. (1) and (2):

$$k''_e = \frac{\mu_{ep}}{\mu_{eo2}} \quad (1)$$

$$k'' - \frac{t_{M2} \times (1 + k''_e) - t_{02}}{t_{02}} \quad (2)$$

where μ_{ep} and μ_{eo2} are the electrophoretic and electroosmotic mobility, which can be obtained respectively from open-tubular CE experiments on a bare capillary (column 1) and from the CEC experiments on the MWNT immobilized capillary (column 2) as follows:

$$\mu_{ep} = \frac{L_1 \times L_{d1}}{V_1} \times \left(\frac{1}{t_{M1}} - \frac{1}{t_{01}}\right)$$

$$\mu_{eo2} = \frac{L_2 \times L_{d2}}{t_{02} \times V_2}$$

where L = total column length, L_d = the distance between the inlet and the detection point, V = applied voltage, t_M = migration time of solute, t_0 = migration time of DMSO. The electrophoretic and chromatographic migration parameters are collected in Table 1. Either the μ_{ep} or k''_e values are negative, which means that the electrophoretic migration of solutes was counter to the cathodic EOF in the borate buffer system (pH 9.55, 30 mM). Although their pK_a values (Urd, 10.0; Guo, 10.0; Thy, 10.2; Thd, 10.5; Ado, 12.4; Cyd, 12.5) [43] are larger than 9.55, some of solutes had migrated towards the anode under the acetate [43], carbonate [44] and borate/diethylamine buffers [40] around pH 9.55 in a CZE mode. A closer inspection of the k''_e values along with the migration order revealed that guanosine in particular exhibited a lesser anodic electrophoretic mobility (-1.8×10^{-4} cm^2 V^{-1} s^{-1}), but eluted later than Thy (−1.9), Ado (−2.4) and Cyd (−2.6). The strong retention of guanosine was caused by its chromatographic interaction with MWNTs immobilized on the stationary phase and also was reflected on the retention factor (k''). In fact, the k'' value (0.86) for the guanosine solute was the highest among the solutes. Guanosine is built from a purine nucleobase, guanine, which consists of nitrogen heterocycles with a double ring that creates an enhancement of π–π interaction with the carbon double bonds in the MWNT structure. Although adenosine also owns a purine moiety, it did not have a high k'' value (0.22). This may suggest that in addition to the π–π interaction, other interactions, such as hydrogen bonding, hydrophobic, and electrostatic interactions with carboxylic groups on the modified MWNT, also contribute to the chromatographic retention.

Regardless of the extent of each interaction, a reversed-phase mechanism could be approved through the addition of an organic modifier, acetonitrile, to the running buffer. As shown in Fig. 6, each solute migrates at a slower rate than its respective migration in Fig. 5. The prolonged migration time was simply caused by the reduced EOF (as shown in Fig. 4), which is not a presentation of a normal-phase mechanism. In fact, the k'' values in the condition with the ACN addition are lower than those without ACN, as the two sets of data in Table 1 are compared for the SiH-CNT2 column. Here, a reversed-phase chromatography exists in the MWNT-based CEC separation.

Table 1
Electrochromatographic properties of nucleosides and thymine in the SiH-CNT2 column.

Migration order	Solutes	Bare fused-silica column[a]		SiH-CNT2 column[b]					
		t_{M1} (min)	$\mu_{ep} \times 10^{-4}$ (cm^2 V^{-1} s^{-1})	t_{M2} (min)	k''_e	k''	W (s)	N (×10^5)	R_s
In the borate buffer, pH 9.55, 30 mM									
1	Thymidine	7.598	−1.3	7.885	−0.18	0.12	7.906	5.7	21
2	Thymine	8.633	−1.9	9.894	−0.26	0.27	3.228	5.4	8.6
3	Adenosine	9.837	−2.4	10.527	−0.33	0.22	5.565	2.1	28
4	Cytidine	10.398	−2.6	13.184	−0.36	0.47	5.655	3.1	10
5	Guanosine	8.484	−1.8	14.302	−0.25	0.86	7.365	2.2	36
6	Uridine	13.134	−3.3	19.264	−0.46	0.82	9.233	2.5	
In the borate buffer (pH 9.55, 30 mM) added with ACN (5%, v/v)									
1	Thymidine	8.079	−1.1	9.363	−0.19	0.04	12.832	3.1	17
2	Thymine	9.272	−1.7	12.143	−0.29	0.18	6.412	2.1	14
3	Adenosine	11.203	−2.3	13.663	−0.41	0.11	7.028	2.2	22
4	Cytidine	11.645	−2.4	16.286	−0.42	0.30	7.410	2.8	13
5	Guanosine	8.896	−1.5	18.188	−0.26	0.84	9.779	2.0	43
6	Uridine	16.848	−3.4	26.798	−0.60	0.49	14.584	1.9	

[a] L_1 = 59.5 cm, Ld_1 = 54.8 cm, 15 kV applied voltage; $\mu_{eo1} = 9.0 \times 10^{-4}$ cm^2 V^{-1} s^{-1} in the condition without ACN modifier and $\mu_{eo1} = 8.4 \times 10^{-4}$ cm^2 V^{-1} s^{-1} in the condition of 5% (v/v) ACN addition; t_{M1}, migration time; μ_{ep}, electrophoretic mobility.

[b] L_2 = 52.7 cm, Ld_2 = 47.7 cm, 10 kV applied voltage; $\mu_{eo2} = 7.3 \times 10^{-4}$ cm^2 V^{-1} s^{-1} in the condition without ACN modifier and $\mu_{eo2} = 5.8 \times 10^{-4}$ cm^2 V^{-1} s^{-1} in the condition of 5% (v/v) ACN addition; t_{M1}, migration time; k''_e, velocity factor; k'', retention factor; W, peak width; N, theoretic plate number; R_s, resolution.

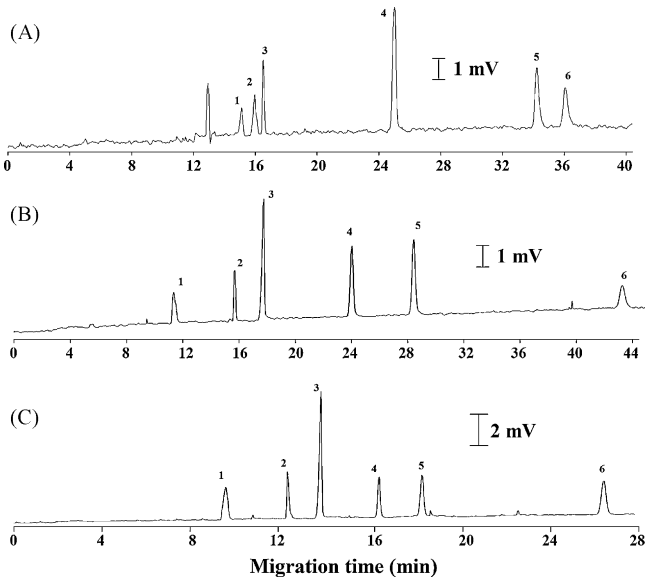

Fig. 6. Electrochromatographic separation of the mixture of nucleosides and thymine under the borate buffers with 5% (v/v) ACN modifier in various MWNT immobilized capillaries. Sample, column, condition, and peak identification are the same as Fig. 5.

3.3. Separation of tetracyclines

Firstly, the four prepared tetracyclines (TCs) were tested by the SiH-CNT2 capillary under the phosphate and borate buffers in the pH range of 7.5–10.5. However, most peaks are broad, rounded, and unresolved. One representative plot is shown in Fig. 7(A). In those cases, the lack of column efficiency and selectivity may result from the inefficient mass transfer and low loadability of recognition ligands on the stationary phase. Thus, increasing the amount of MWNT groups attached on the stationary phase would probably increase the column performance. This could be done simply by replacing the SiH-CNT2 column with the SiH-CNT2×5 one. Accordingly, the trial column performed as expected, with improved separation performance. A direct comparison between these two columns under the same buffer (borate, pH 9.51, 50 mM) and electrical field is depicted in Fig. 7(A) and (B).

The performance of the SiH-CNT2×5 column at other pH levels is presented in Fig. 8. Among of them, the trace shown in Fig. 8(B) at pH 10.0 is especially satisfying. Those traces, including the results at pH 10.0 and 10.51, even resolved the peaks of chlortetracycline (peak 2) and its isotetracycline derivative (peak 2′), which is formed with a γ-lactone structure in basic media. The peak 2′ appears in the buffers with higher pH values, such as those in Fig. 7, Fig. 8(B) and (C) (pH ≥ 9.51), but not in Fig. 8(A) (pH = 9.06). Moreover, a higher peak area ratio of peak 2′ to peak 2 could also be found in the higher pH buffers, as the extent of lactonization happened during the CEC progressing in the SiH-CNT2×5 column could be indexed by this ratio. The other three TCs solutes do not have the 6-OH group in their structures, so no respective isotetracycline would be produced in an alkali media.

Table 2 shows the electrochromatographic properties of TCs migrating in the conditions of Fig. 8(B). Here, these TCs solutes bear nearly two negative charges at pH 10.00 (MNC: pK_a = 2.8, 5.0, 7.8, 9.5 for H_4A^{+2}; CTC: pK_a = 3.33, 7.55, 9.33 for H_3A^+; MTC: pK_a = 3.5,

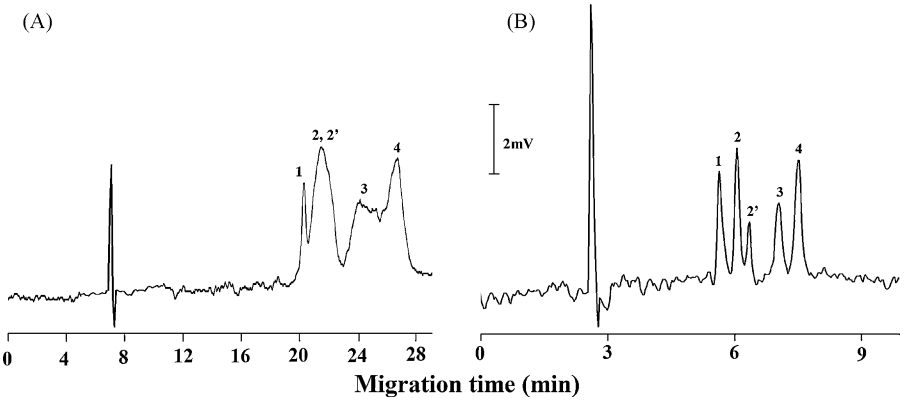

Fig. 7. Electrochromatographic separation of tertracyclines in various MWNT immobilized capillaries. Column: (A) SiH-CNT2, 59.5 cm (54.8 cm) × 75 μm I.D.; (B) SiH-CNT2×5, 36.4 cm (31.4 cm) × 75 μm I.D. Sample: concentration, 0.05 mg/mL; hydrostatic injection, 15 cm, 8 s; detection, 355 nm. Condition: BGE, borate buffer, pH 9.51, 0.05 M; applied voltage, 10 kV. Peak identification: (1) MNC, (2) CTC, (2′) iso-CTC, (3) MTC, and (4) DC.

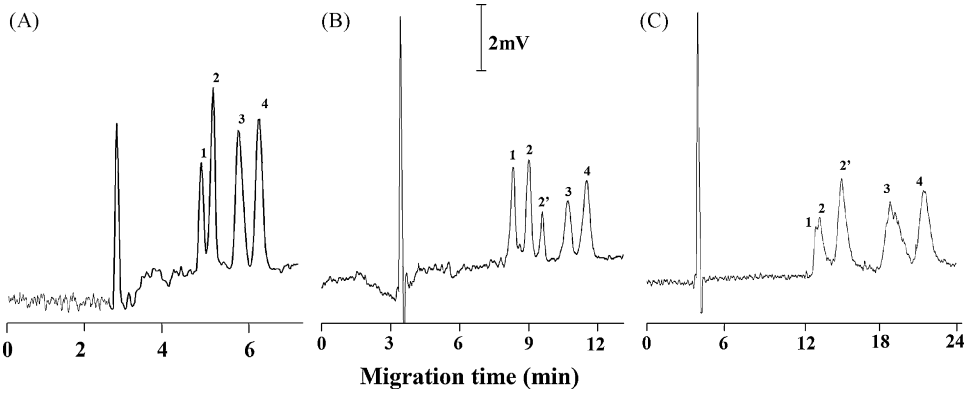

Fig. 8. Electrochromatographic separation of tertracyclines at various pH levels in SiH-CNT2×5 capillary. BGE condition: (A) pH 9.06; (B) pH 10.00; (C) 10.51 (borate buffer, 0.05 M). Applied voltage: 10 kV. Sample, column, and peak identification are the same as Fig. 7.

Table 2
Electrochromatographic properties of tetracyclines in the SiH-CNT2×5 column.

Migration order	Solutes	Bare fused-silica column[a,b]		SiH-CNT2×5 column[a,c]					
		t_{M1} (min)	$\mu_{ep} \times 10^{-4}$ ($cm^2\ V^{-1}\ s^{-1}$)	t_{M2} (min)	k''_e	k''	W (s)	N ($\times 10^4$)	R_s
1	Minocycline	32.734	−6.5	8.402	−0.58	1.1	13.170	2.3	3.1
2	Chlortetracycline	34.862	−6.6	9.080	−0.58	1.2	13.500	2.6	3.1
2′	Iso-chlortetracycline	36.678	−6.6	9.652	−0.59	1.3	8.756	7.0	4.9
3	Methacycline	42.067	−6.8	10.788	−0.61	1.6	19.141	1.8	2.5
4	Doxycycline	38.829	−6.7	11.623	−0.60	1.7	20.288	1.9	

[a] In the conditions of borate buffer, 50 mM, pH 10.00, and 10 kV applied voltage.
[b] $L_1 = 59.5$ cm, $Ld_1 = 54.8$ cm, $\mu_{eo1} = 8.1 \times 10^{-4}\ cm^2\ V^{-1}\ s^{-1}$.
[c] $L_2 = 36.4$ cm, $Ld_2 = 31.4$ cm, $\mu_{eo2} = 1.2 \times 10^{-3}\ cm^2\ V^{-1}\ s^{-1}$.

7.6, 9.2 for H_3A^+; DC: $pK_a = 3.02, 7.97, 9.15$ for H_3A^+) [45–47] and exhibit high μ_{ep} values ($\geq 6.453 \times 10^{-4}\ cm^2\ s^{-1}\ V^{-1}$). Although the μ_{ep} values are close to each other, a large difference in k'' values may generate appreciable resolutions ($R_s \geq 2.54$). In comparison with the k'' values in Table 1, the greater k'' of the TCs solutes may result from the high loadability of MWNTs in the SiH-CNT2×5 capillary, aside from the solutes' partitioning characteristics. Furthermore, raising the EOF by shortening the column length at the same applied voltage and relying on the SiH-CNT2×5 column with an intrinsic high μ_{eo} value would also contribute to the enhanced resolution.

4. Conclusions

This study took advantage of the high reactivity of carbon-atom pentagons in the CNT structure. The bonded-phase CEC capillaries were successfully completed by hydrosilation of non-acid- or acid-treated MWNTs with the silica-hydride capillary. In addition to SEM and ATR-IR, these CEC capillaries were characterized by the EOF responses driven from the carboxylate groups on the MWNTs to the pH levels of buffers and to the addition of ACN modifier. The chromatographic contribution to the CEC mechanism was separated from the electrophoretic migration of test solutes (a mixture of nucleosides and thymine) and was identified as a reversed-phase chromatography and a π–π interaction in the HNO_3-HCl treated capillary. It is suggested that the conditions of hydrosilation be adjusted for the CEC separation of specific samples; for example, tetracyclines were well separated in the capillary with a higher loadability of MWNTs. Certainly, further modification of MWNTs before or after the hydrosilation would be a feasible approach to advanced studies.

Acknowledgements

Support of this work by the National Science Council of Taiwan (NSC-98-2113-M-039-003-MY3) is gratefully acknowledged.

Appendix A. Supplementary data

Supplementary data associated with this article can be found, in the online version, at doi:10.1016/j.chroma.2009.12.018.

References

[1] E. Guihen, J.D. Glennon, J. Chromatogr. A 1044 (2004) 67.
[2] C.P. Kapnissi-Christodoulou, X. Zhu, I.M. Warner, Electrophoresis 24 (2003) 3917.
[3] J. Ou, J. Dong, X. Dong, Z. Yu, M. Ye, H. Zou, Electrophoresis 28 (2007) 148.
[4] X. Dong, R. Wu, J. Dong, M. Wu, Y. Zhu, H. Zou, Electrophoresis 30 (2009) 141.
[5] J.J. Pesek, M.T. Matyska, V. Salgotra, Electrophoresis 29 (2008) 3842.
[6] L. Xu, X.Y. Dong, Y. Sun, Electrophoresis 30 (2009) 689.
[7] S.S. Zhang, M. Macka, P.R. Haddad, Electrophoresis 27 (2006) 1069.
[8] J. Ruiz-Jimenez, R. Kuldvee, J. Chen, K. Öörni, P. Kovanen, M.-L. Riekkola, Electrophoresis 28 (2007) 779.
[9] K. Vainikka, J. Chen, J. Metso, M. Jauhiainen, M.L. Riekkola, Electrophoresis 28 (2007) 2267.
[10] X.L. Dong, R.A. Wu, M.H. Wu, J. Dong, M. Wu, Y. Zhuz, H. Zou, Electrophoresis 29 (2008) 3933.
[11] Y.L. Hsieh, T.H. Chen, C.P. Liu, C.Y. Liu, Electrophoresis 26 (2005) 4089.
[12] R.H. Baughman, A.A. Zakhidov, W.A. de Heer, Science 297 (2002) 787.
[13] V. Sgobba, D.M. Guldi, Chem. Soc. Rev. 38 (2009) 165.
[14] M. Valcárcel, S. Cárdenas, B.M. Simonet, Y. Moliner-Martínez, R. Lucena, Trends Anal. Chem. 27 (2008) 34.
[15] T. Cserháti, Biomed. Chromatogr. 23 (2009) 111.
[16] Z. Zhang, Z. Wang, Y. Liao, H. Liu, Sep. Sci. 29 (2006) 1872.
[17] V.R. Reida, M. Stadermannb, O. Bakajin, R.E. Synovec, Talanta 77 (2009) 1420.
[18] Y. Moliner-Martínez, S. Cárdenas, B.M. Simonet, M. Valcárcel, Electrophoresis 30 (2009) 169.
[19] J.H.T. Luong, P. Bouvrette, Y. Liu, D.Q. Yang, E. Sacher, J. Chromatogr. A 1074 (2005) 187.
[20] Y. Li, Y. Chen, R. Xiang, D. Ciuparu, L.D. Pfefferle, Cs. Horváth, J.A. Wilkins, Anal. Chem. 77 (2005) 1398.
[21] X. Weng, H. Bi, B. Liu, J. Kong, Electrophoresis 27 (2006) 3129.
[22] L. Sombra, Y. Moliner-Martínez, S. Cárdenas, M. Valcárcel, Electrophoresis 29 (2008) 3850.
[23] Z. Jia, Z. Wang, C. Xu, J. Liang, B. Wei, D. Wu, S. Zhu, Mater. Sci. Eng. 271 (1999) 395.
[24] S.J. Park, M.S. Cho, S.T. Lim, H.J. Choi, M.S. Jhon, Macro. Rapid Commun. 24 (2003) 1070.
[25] C.H. Chu, E. Jonsson, M. Auvinen, J.J. Pesek, J.E. Sandoval, Anal. Chem. 65 (1993) 808.
[26] J.J. Pesek, M.T. Matyska, J. Liq. Chromatogr. Relat. Technol. 29 (2006) 1105.
[27] J.J. Pesek, M.T. Matyska, S. Sentellas, M.T. Galceran, M. Chiari, G. Pirri, Electrophoresis 23 (2002) 2982.
[28] J.J. Pesek, M.T. Matyska, J. Sep. Sci. 27 (2004) 1285.
[29] J.-L. Chen, Electrophoresis 30 (2009) 3855.
[30] J.-L. Chen, J. Chromatogr. A 1216 (2009) 6236.
[31] R.M. Silverstein, F.X. Webster, D. Kiemle (Eds.), Spectrometric Identification of Organic Compounds, 7th ed., John Wiley & Sons, New Jersey, 2005.
[32] X. Kang, W. Ma, H.-L. Zhang, Z.-G. Xu, Y. Guo, Y. Xiong, J. Appl. Polym. Sci. 110 (2008) 1915.
[33] W. Zou, Z. Du, Y. Liu, X. Yang, H. Li, C. Zhang, Compos. Sci. Technol. 68 (2008) 3259.
[34] J. Liu, A.G. Rinzler, H. Dai, H. Hafner, R.K. Bradley, P.J. Boul, A. Lu, T. Iverson, K. Shelimov, C.B. Huffman, F. Rodriguez-Macias, Y. Shon, T.R. Lee, D.T. Colbert, R.E. Smalley, Science 280 (1998) 1253.
[35] H. Jankowska, A. Swiatkowski, J. Choma (Eds.), Active Carbon, Ellis Horwood Ltd., New York, 1991.
[36] X.-H. Chen, C.-S. Chen, Q. Chen, F.-Q. Cheng, G. Zhang, Z.-Z. Chen, Mater. Lett. 57 (2002) 734.
[37] J.-L. Chen, Electrophoresis 27 (2006) 729.
[38] L. Xu, Y. Sun, Electrophoresis 28 (2007) 1658.
[39] Ph. Schmitt-Kopplin, N. Hertkorn, A.W. Garrison, D. Freitag, A. Kettrup, Anal. Chem. 70 (1998) 3798.
[40] M. Haunschmidt, W. Buchberger, C.W. Klampfl, J. Chromatogr. A 1213 (2008) 88.
[41] A.S. Rathore, Cs. Horváth, J. Chromatogr. A 743 (1996) 231.
[42] A.S. Rathore, Cs. Horváth, Electrophoresis 23 (2002) 1211.
[43] T. Furumoto, T. Furumoto, M. Sekiguchi, T. Sugiyama, H. Watarai, Electrophoresis 22 (2001) 3438.
[44] S.E. Geldart, P.R. Brown, J. Chromatogr. A 831 (1999) 123.
[45] A.G. Butterfield, D.W. Hughes, N.J. Pound, W.L. Wilson, Antimicrob. Agents Chemother. 4 (1973) 11.
[46] Z. Qiang, C. Adams, Water Res. 38 (2004) 2874.
[47] G.S. Avery (Ed.), In Drug Treatment Principles and Practice of Clinical Pharmacology and Therapeutics, 2nd ed., Adis Press, Sydney, 1980.